

Advanced Materials Research

Eduardo Alves

The Advanced Materials Research Group (GIMA) operates most of the experimental facilities at the Ion Beam Laboratory (IBL). The IBL is equipped with a 2.5 MV Van de Graaff accelerator with a nuclear microprobe and external beam facility; a 3 MV tandem accelerator with a 30 μm lateral resolution Accelerator Mass Spectrometry (AMS) system; a high flux Danfysik S1090 ion implanter.

The group explores and develop ion beam techniques to study advanced materials with high technological impact, e.g. wide band gap semi-conductors nanostructures, oxides and functional materials in collaboration with a long list of other groups. Among the wide band gap materials our major interests is focused on III-nitrides and ZnO. These alloys are the base of an emerging class of optoelectronic devices operating in the visible wavelength range of the electromagnetic spectrum being under intense research worldwide. Our work aims at the optimization of the implantation conditions of magnetic and optically active dopants in these materials. In addition an intense research on the structural properties and Rare Earth doping of GaN/AlN QD layers continued in collaboration with Universities of Aveiro, Grenoble and Strathclyde.

The work in oxides aims at modification of the optical and structural properties of $\alpha\text{-Al}_2\text{O}_3$ as well as the study of magnetic doping of ZnO by ion implantation. The potential of these materials for spintronics applications is being investigated with University of Aveiro and Faculty of Sciences of University of Lisboa.

Taking advantage of the versatility of ion beam techniques to study thin films and multilayers, important work continued on the characterisation of magnetic thin films for magnetic spin valves, tunnel junctions, and functional oxynitride coatings, in

collaboration with INESC, University of Minho and New University of Lisbon.

The activities under the technology programme of the European Fusion Development Agreement (EFDA), in association with Instituto de Plasmas e Fusão Nuclear (IPFN) was focused on the study beryllium intermetallics and the study of surface erosion and redeposition processes as well as ^2H retention in JET tiles.

Training and Education continued as a major commitment of the group through the supervision of M.Sc. and Ph.D. thesis.

All the referred activities are funded by projects, either European or National (FCT), in collaboration with other Institutions. Of particular importance are the projects funded by the EC, "FEMaS-Fusion Energy Material Science", EURATON 7th Framework Programme for Nuclear Research and Training, Grant agreement No 224752-CA, (2008-2011) and "Support of Public and Industrial Research Using Ion Beam Technology (SPIRIT)", Grant agreement No 227012-CP-CSA-Intra (starting date 2009/03/01) and EFDA JET Technology Workprogramme JW10-FT-3.59.

The external collaborations allowed a continuous exchange of expertise and mobility of researchers, a key condition to keep the scientific activity of the group at the forefront of research and its international recognition in the field of processing and characterization of advanced materials with ion beams.

Publications (peer reviewed journals): 1 book chapter and 58 papers.

Conference and workshop contributions: 2 invited, 13 oral and 23 posters.

Running projects: 20

Research Team

Researchers^(*)

E. ALVES, Principal (Group Leader)
R.C. SILVA, Principal
L.C. ALVES, Aux. (75%)
U. WAHL, Principal (85%)
K. LORENZ, Aux. (90%)
V. DARAKCHIEVA, Aux.
V. CORREGIDOR., Aux.
A. R. RAMOS, Aux. (15%)
A. KLING, Aux. (15%)
N.P. BARRADAS, Aux. (15%)
A.C. MARQUES, Post-Doc, FCT grant
N. FRANCO, Post-Doc, FCT grant
R. MARTINS Post-Doc, FCT grant

P.A. MIRANDA JAÑA Post-Doc. Fellow
under the EU SPIRIT Project

Students

B.M. NUNES,
I. FIALHO, M.Sc
L.M. PEREIRA, Ph.D. (FCT)
M.A.D. MERCIER, IST Student
M. XIE
N. CATARINO
S. MAGALHÃES, Ph.D. (FCT)
S. MIRANDA

Collaborators

A. RODRIGUES

C.P. MARQUES
J.V. PINTO
J.G. LOPES
M. VILARIGUES
R. MATEUS

Technical Personnel

J. ROCHA
F. BAPTISTA
P. PEREIRA

(*) Also members of CFNUL.

Lattice site location of optical centres in GaN:Eu light emitting diode material

K. Lorenz, E. Alves, I. S. Roqan¹, K. P. O'Donnell¹, A. Nishikawa², Y. Fujiwara², and M. Boćkowski³

Introduction

Europium doped GaN is a promising material for red light emitting diodes (LEDs) and lasers [1]. GaN:Eu was grown by organometallic vapour phase epitaxy (OMVPE) at temperatures (T_G) from 900 to 1100 °C. Rutherford backscattering spectrometry/Channelling (RBS/C) was performed to investigate crystal quality, composition and Eu incorporation site [2]. Optical activity was assessed by photoluminescence.

Results

RBS/C minimum yields below 3% reveal the excellent crystal quality of all five investigated layers (Fig. 1). Eu incorporation is influenced by temperature with the highest concentration found for growth at 1000 °C.

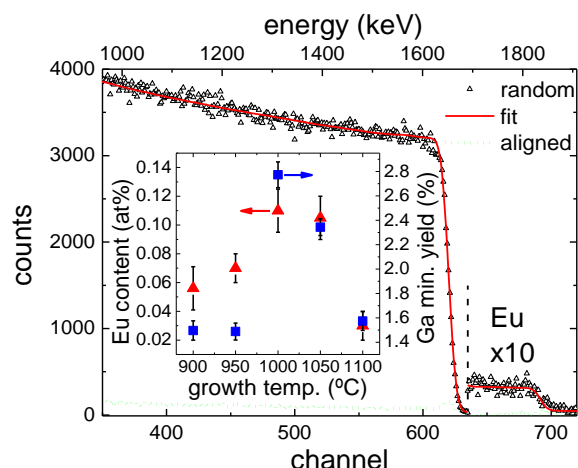


Fig. 1: RBS/C random and $\langle 0001 \rangle$ aligned spectra and the fit to the random spectrum of the sample grown at 1000 °C. The inset shows Eu concentration and Ga minimum yield as a function of T_G for all in situ doped samples.

Fig. 2 shows full angular RBS/C scans across the $\langle 0001 \rangle$ and the $\langle 10\bar{1}1 \rangle$ axes for two samples. In all samples, Eu is incorporated entirely on substitutional Ga sites with a slight displacement which is highest (~ 0.2 Å) in the sample grown at 900 °C and mainly directed along the c-axis.

Photoluminescence (PL) measurements reveal that the dominant optical Eu^{3+} centres in samples grown at higher temperatures are identical to ion-implanted samples after high temperature and pressure annealing (Fig. 3). They are attributed to isolated, substitutional Eu [3]. The sample grown at 900 °C, on the other hand, showed only a weak and broad red emission without the typical sharp lines. This, and the fact that Eu is found displaced from the substitutional site in this sample, was tentatively explained by the formation of Eu clusters promoted by a low diffusion length of adatoms at low growth temperatures. Finally, the red PL intensity of the best in situ doped sample is 20 times stronger than that of a low fluence implanted and fully annealed sample while the number of Eu ions is approximately 400 times larger,

pointing to a significant potential for optimization of luminescence efficiency in future GaN:Eu based LEDs.

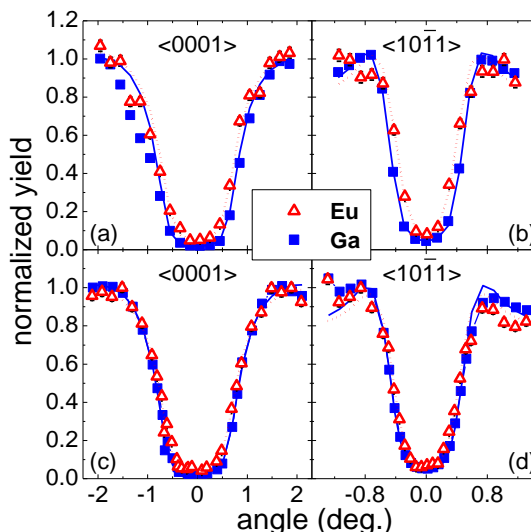


Fig. 2: Full angular scans (symbols) and fits (lines) for Eu and Ga across the $\langle 0001 \rangle$ and the $\langle 10\bar{1}1 \rangle$ axes for samples grown at 900 °C (a and b) and at 1000 °C (c and d).

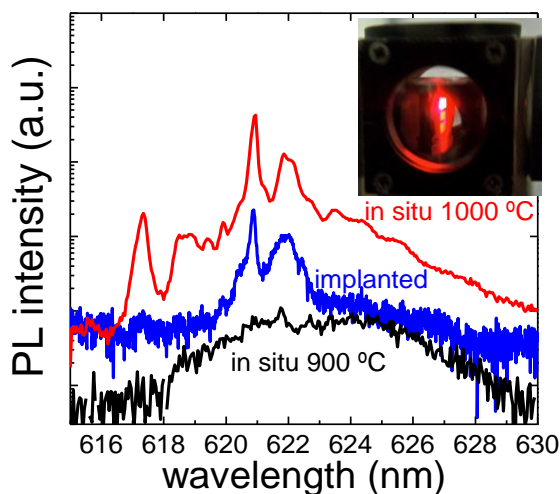


Fig. 3: PL spectra ($\lambda_{exc}=348$ nm) of samples grown at 900 and 1000 °C compared to an Eu ion implanted sample. The inset photo shows the intense red Eu emission.

- A. Nishikawa et al., Appl. Phys. Express 2, 071004 (2009).
 K. Lorenz et al., Appl. Phys. Lett. 97, 111911 (2010).
 I. S. Roqan et al., Phys. Rev. B 81, 085209 (2010).

¹ University of Strathclyde, Glasgow, U.K.

² Division of Materials and Manufacturing Science, Osaka University, Japan.

³ Institute of High Pressure Physics, Polish Academy of Sciences Warsaw, Poland.

Lattice site location of optical centres in GaN:Eu light emitting diode material grown by OMVPE*K. Lorenz, E. Alves, I. S. Roqan¹, K. P. O'Donnell¹, A. Nishikawa², Y. Fujiwara², and M. Boćkowski³*

Eu-doped GaN was grown by organometallic vapour phase epitaxy (OMVPE) at temperatures from 900 to 1100 °C. Eu incorporation is influenced by temperature with the highest concentration found for growth at 1000 °C. In all samples, Eu is incorporated entirely on substitutional Ga sites with a slight displacement which is highest (~0.2 Å) in the sample grown at 900 °C and mainly directed along the c-axis. The dominant optical Eu³⁺ centres in samples grown at higher temperatures are identical to ion-implanted samples after high temperature and pressure annealing. They are attributed to isolated, substitutional Eu. The sample grown at 900 °C, on the other hand, showed only a weak and broad red emission without the typical sharp lines. This and the fact that Eu is found displaced from the substitutional site in this sample was tentatively explained by the formation of Eu clusters promoted by a low diffusion length of adatoms at low growth temperatures. Finally, the red PL intensity of the best *in situ* doped sample is 20 times stronger than that of a low fluence implanted and fully annealed sample while the number of Eu ions is approximately 400 times larger, pointing to a significant potential for optimization of luminescence efficiency in future GaN:Eu based LEDs.

¹ Department of Physics, SUPA, University of Strathclyde, Glasgow, G4 0NG, U.K.² Division of Materials and Manufacturing Science, Graduate School of Engineering, Osaka University, Osaka, Japan.³ Institute of High Pressure Physics Polish Academy of Sciences 01-142 Warsaw, Poland.**Analysis of Rutherford Backscattering Spectrometry spectra for the determination of the InN content and its uncertainty of Al_{1-x}In_xN films grown on GaN/sapphire templates***S. Magalhães, N. P. Barradas, N. Franco, E. Alves, I. M. Watson¹, K. Lorenz*

Simulation softwares, such as NDF, RUMP or SIMNRA, are routinely used for the analysis of Rutherford Backscattering Spectrometry (RBS) spectra. In some cases, however, a manual analysis of RBS spectra may be more convenient and allows a more rigorous determination of the uncertainties in the derived sample composition. Al_{1-x}In_xN/GaN films represent such a case, in which the Al/In ratio, and therefore the InN molar fraction *x*, can be easily determined by integrating the areas in the spectrum corresponding to In and Al. In such an analysis, uncertainties in the charge, stopping powers and energy calibration are eliminated and the main sources of error are the counting statistics, background subtraction as well as uncertainties in beam energy and geometry of the measurements which can be easily taken into account. The main source of error in the RBS analysis of AlInN/GaN is the subtraction of the background below the Al-signal since it is superimposed to the Ga-signal of the GaN buffer layer. The necessity of a fast analysis gave the motivation of elaborating a data analysis program which automates the background subtraction and calculates the InN molar fraction and its uncertainty. The proposed method determines the Al-area using a third degree polynomial to fit the Ga-background which is then subtracted. A large number of different regions of interests are used in which the polynomial fit is performed and from which the error in the Al-area is estimated. A linear fit is used for subtracting the background below the In-signal which is mainly caused by pile-up. Various tests were performed to evaluate the method's validity. A manual analysis to a simulated "theoretical spectrum", using detector resolution and pile-up typical for the experiments, yields excellent agreement. The estimated errors in the InN molar fraction for samples with *x*~18% are around 0.5-1% absolute.

¹ Institute of Photonics, SUPA, University of Strathclyde, G40NW Glasgow, U.K.**Structural and optical characterization of Europium implanted GaN quantum dots***S. Magalhães, M. Peres¹, V. Fellmann², B. Daudin², E. Alves, A. J. Neves¹, T. Monteiro¹, K. Lorenz*

Self-assembled GaN quantum dots (QDs) stacked in superlattices (SL) with AlN spacer layers were implanted with Europium ions to fluences of 10¹³, 10¹⁴, and 10¹⁵ cm⁻². Post-implant annealing was performed between 1000 °C and 1200 °C in nitrogen. The damage level introduced in the QDs by the implantation stays well below that of thick GaN epilayers. For the lowest fluence, the structural properties remain unchanged after implantation and annealing while for higher fluences the implantation damage causes an expansion of the SL in the [0001] direction which is only partly reversed after thermal annealing. Nevertheless, in all cases, the SL quality remains very good after implantation and annealing. Eu ions are incorporated preferentially into near-substitutional cation sites. Eu³⁺ luminescence was observed in all samples with the most intense emission assigned to the ⁵D₀→⁷F₂ transition in the red spectral region. Optically active Eu centres in both GaN QD and AlN layers could be identified. For low implantation fluence the Eu centres inside GaN QD are dominant while for high fluences the emission arises from Eu in the AlN layers. The annealing temperature, on the other hand, does not cause any change in the local environment of the Eu-ions.

¹ Departamento de Física & I3N, Universidade de Aveiro, 3810-193 Aveiro, Portugal.² CEA-CNRS Group "NanoPhysique et SemiConducteurs", CEA-Grenoble, France.

Structural and optical characterization of Eu-implanted non-polar and polar GaN

N. Catarino, E. Nogales¹, B. Méndez¹, E. Alves, K. Lorenz

Europium (Eu) ions were implanted into non-polar a-plane (11-20) gallium nitride (GaN) films grown on r-plane sapphire with fluences ranging from 1×10^{14} to 4×10^{15} cm⁻² at room temperature (RT). Results are compared with similarly implanted polar c-plane (0001) GaN films. Structural and optical characterizations of the samples were performed using Rutherford backscattering spectrometry and channelling (RBS/C) and cathodoluminescence (CL) spectroscopy. RBS/C measurements for the as-implanted samples reveal similar damage formation for both materials with two different damage regions, one at the surface and one deeper in the crystal. For the highest fluences the channelling effect in the surface region is completely suppressed indicating amorphisation or nanocrystallization of this layer. The damage in the bulk stays well below the random level and is substantially lower for a-plane GaN, in particular for high fluences. In both cases, Eu is incorporated on near-substitutional Ga-sites. After annealing at 1000 °C both materials show good recovery of the crystal quality and the Eu ions are optically activated. Both, a- and c-plane GaN films show similar behavior, the CL intensity is increasing steeply for implantation from 1×10^{14} to 2×10^{15} cm⁻²; for the highest fluences the CL intensity is decreasing again due to the severe structural damage.

¹ Dpto. Física de Materiales, Universidad Complutense de Madrid, 28040 Madrid, Spain.

Optical doping of AlN micro- and nanorods by rare earth ions

V. Darakchieva, M.-Y. Xie,¹ R. Yazdi,² R. Yakimova,¹ J. Rodrigues,² T. Monteiro,² E. Alves, K. Lorenz

The doping of III-nitrides with optically active rare earth (RE) ions offers an attractive route to an all-nitride light emitting technology covering the entire wavelength range from UV to IR. The possibility to mix colours and achieve white light opens opportunities for efficient solid state lighting with high energy saving potential. The most challenging issue to solve on the way to produce RE doped devices is the efficiency, which is strongly dependent on the excitation cross-section. A promising approach may be the RE doping of nitride nanostructures where the carrier confinement can increase the excitation cross-section.

We performed RE doping of AlN microrods and nanorods in order to achieve emission in the visible. The AlN micro- and nanorods (Fig.1) were implanted with Eu (red), Tm (blue) and Er (green) RE ions and subsequently annealed in order to activate the ions and remove the crystal damage. The structural properties of the AlN rods have been studied before and after implantation and annealing. Cathodoluminescence measurements reveal strong emission lines from the RE ions at room temperature (Fig.1). The principal ⁵D₀ → ⁷F₂ red transition is identified in the AlN rods implanted with Eu. A weak ¹G₄ → ³H₆ transition is detected in the blue spectral region of the Tm doped AlN sample, while the higher lying blue line (¹D₂ → ³F₄), dominant in AlGaN alloys, is absent. The spectrum is dominated by the IR transition at around 800 nm. The Er doped AlN rods revealed very intense transitions in the red possibly due to an unintentional co-implantation with Eu. The visible green Er emission is seen only weakly in the 530 nm region. We are currently investigating the possibility of energy transfer from Er to Eu in these structures, as well as the RE ion incorporation and optically active centres.

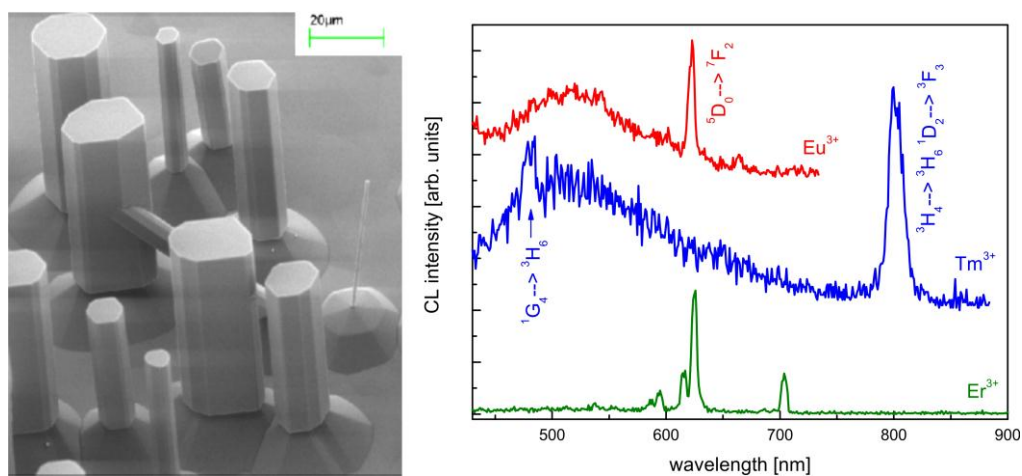


Fig. 1 - Scanning electron micrograph of the AlN micro- and nanorods implanted with different RE ions and their room temperature cathodoluminescence spectra.

¹ Department of Physics, Chemistry and Biology, Linköping University, SE-581 83 Linköping, Sweden.

² Departamento de Física, Universidade de Aveiro, 3810-193 Aveiro, Portugal.

Ion implantation of Cd and Ag into AlN and GaN

S. M. C. Miranda, E. Alves, K. Lorenz

Group III nitrides are promising and competitive materials for optoelectronic applications due to their wide and direct band gap. Although GaN and especially AlN show strong radiation damage resistance, the use of ion implantation in device processing still requires more knowledge on damage formation and appropriate post-implant annealing procedures. GaN and AlN thin films, grown by hydride vapor phase epitaxy on sapphire, were ion implanted at room temperature with cadmium (Cd) and silver (Ag), with fluences ranging from 1×10^{13} to 1.5×10^{15} cm^{-2} at 150 keV. The as-implanted samples were annealed at 950 °C in a tube furnace under nitrogen (N) flow for 10 or 20 minutes, for Cd and Ag respectively. A proximity cap was used to prevent N from out-diffusing during the annealing. The samples were characterized by Rutherford Backscattering Spectrometry and Channelling and X-ray Diffraction measurements. The results indicate that implantation damage could be fully removed for the lowest fluences while for higher fluences the crystal quality was only partially recovered. Cd is found incorporated in substitutional cation sites (Al or Ga) while Ag is somewhat displaced from the substitutional position, probably due to the higher implantation damage. The substitutional fraction of Ag in AlN increases after annealing.

Unintentional incorporation of hydrogen in InN: diffusion kinetics and effect of surface orientation

V. Darakchieva¹, K. Lorenz, S.M.C. Miranda, N. P. Barradas, E. Alves, D. Rogala,² H.-W. Becker,² S. Ruffenach,³ O. Briot,³ W. J. Schaff,⁴ C.L. Hsiao,⁵ L.C. Chen,⁵ L.W. Tu,⁶ T. Yamaguchi,⁷ Y. Nanishi⁷

Control of doping in InN and related alloys remains one of the most challenging issues on the way to develop the potential of these materials in new advanced photovoltaic and light emitting device applications. We studied InN films with (0001), (000-1), (10-11) and (11-20) surface orientations grown by molecular beam epitaxy (MBE) and metalorganic vapor phase epitaxy (MOVPE). The H depth profiles in the films are measured by elastic recoil detection analysis and nuclear reaction analysis. All films revealed enhanced H concentrations at their surfaces and significant H amounts in the bulk sufficient to explain the observed free electron concentrations in the films. We have established scaling between H and free electron concentrations in c-plane InN grown by MBE evidencing the major role of H for the unintentional n-type conductivity in this case. The bulk H concentration seems to be dependent on the polarity of the MBE films being lowest in the In-polar, intermediate in the N-polar and semipolar, and highest in the nonpolar InN films (Fig.1). We find similar H areal densities at the (0001), (000-1) and (1-101) surfaces, while nonpolar InN surfaces incorporate much higher amounts of H (Fig.1). Thermal annealing at 350°C in N₂ results in decrease of the H levels with comparable bulk/surface concentrations of H in the polar and semipolar MBE films. However, the H contents in the a-plane MBE films still remain significantly higher after the annealing. We also found a direct evidence for the major role H as a n-type dopant in MOVPE InN based on our annealing studies.

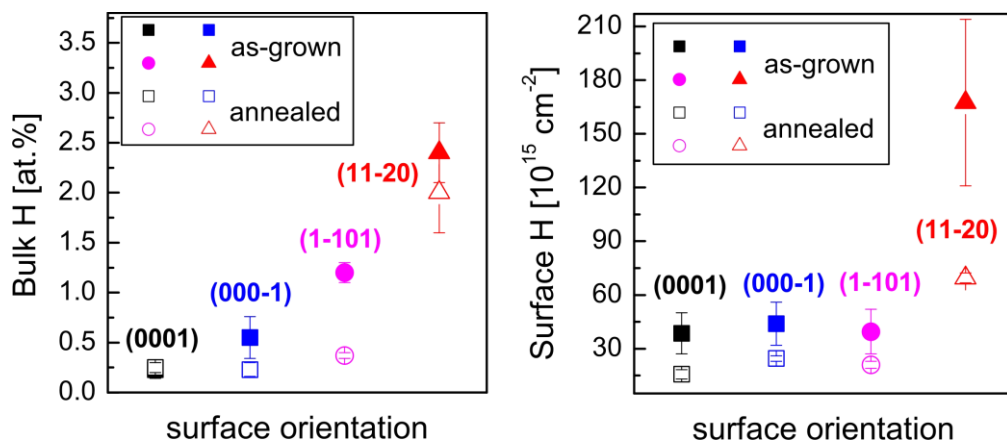


Fig. Bulk and surface H concentrations in four MBE InN films with different surface orientations grown in the same growth equipment.

¹ IFM, Linköping University, SE-581 83 Linköping, Sweden.

² Ruhr-Universität Bochum, Germany.

³ Groupe d'Etude des Semiconducteurs, CNRS, Université Montpellier II, 34095 Montpellier, France.

⁴ Department of Electrical and Computer Engineering, Cornell University, Ithaca, NY 14853, USA.

⁵ Center for Condensed Matter Sciences, National Taiwan University, Taipei 106, Taiwan, ROC.

⁶ National Sun Yat-Sen University, Kaohsiung 80424, Taiwan, ROC.

⁷ Department of Photonics, Ritsumeikan University, Shiga 525-8577, Japan.

Structural anisotropy of nonpolar InN films

V. Darakchieva, M.-Y. Xie,¹ N. Franco, E. Alves, C. L. Hsiao,³ L. C. Chen,² L. W. Tu,³ Y. Takagi,⁴ T. Yamaguchi,⁴ Y. Nanishi⁴

We performed detailed study of the structural characteristics of molecular beam epitaxy grown nonpolar InN films with a- and m-plane surface orientations on r-plane sapphire and (100) γ -LiAlO₂, respectively, and semipolar (10-11) InN grown on r-plane sapphire. The on-axis rocking curve (RC) widths were found to exhibit anisotropic dependence on the azimuth angle with minima at InN [0001] for the a-plane films, and maxima at InN [0001] for the m-plane and semipolar films. The finite size of the crystallites and extended defects are suggested to be the dominant factors determining the RC anisotropy in a-plane InN, while surface roughness and curvature could not play a major role. We furthermore suggest strategy to reduce the anisotropy and magnitude of the tilt and minimize defect densities in a-plane InN films. In contrast to the nonpolar films, the semipolar InN was found to contain two domains nucleating on zinc-blende InN(111)A and InN(111)B faces. These two wurtzite domains develop with different growth rates, which was suggested to be a consequence of their different polarity. Both, a- and m-plane InN films have basal stacking fault densities similar or even lower compared to nonpolar InN grown on free-standing GaN substrates, indicating good prospects of heteroepitaxy on foreign substrates for the growth of InN-based devices.

¹ IFM, Linköping University, Sweden.

² Center for Condensed Matter Sciences, National Taiwan University, Taiwan.

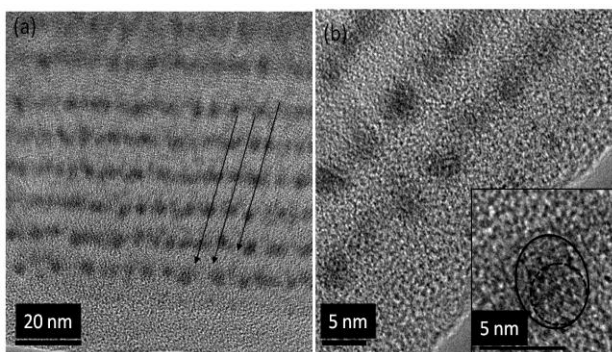
³ Department of Physics, National Sun Yat-Sen University, Taiwan.

⁴ Department of Photonics, Ritsumeikan University, Japan.

Structural study of Si_{1-x}Ge_x nanocrystals embedded in SiO₂ films

S.R.C. Pinto¹, R.J. Kashtiban³, A.G. Rolo¹, M. Buljan², A. Chahboun^{1,4}, U. Bangert³, N.P. Barradas, E. Alves and M.J.M. Gomes¹

The structural properties of Si_{1-x}Ge_x nanocrystals formed in an amorphous SiO₂ matrix by magnetron sputtering deposition were investigated. The influence of deposition parameters on nanocrystal size, shape, arrangement and internal structure was examined by X-ray diffraction, Raman spectroscopy, grazing incidence small angle X-ray scattering, high resolution transmission electron microscopy and ion beam analysis. We found conditions for the formation of spherical Si_{1-x}Ge_x nanocrystals with average sizes between 3 and 13 nm, uniformly distributed in the matrix. In addition we have shown the influence of deposition parameters on average nanocrystal size and Ge content x .



¹ Physics Department, University of Minho, 4710 — 057 Braga, Portugal.

² Charles University in Prague, Ke Karlovu 5, 121 16 Prague, Czech Republic, Ruđer Bošković Institute, Bijenička cesta 54, Croatia.

³ Nanostructured Materials Research Group, School of Materials, The University of Manchester, P.O. Box 88, Manchester, M1 7HS, UK.

⁴ Physics Department, Dhar Mehraz Sciences Faculty, BP 1796, Fès, Morocco.

Effect of nitrogen on the GaAs_{0.9-x}N_xSb_{0.1} dielectric function from the nir-infrared to the ultraviolet

N. Ben Sedrine, C. Bouhafs¹, J. C. Harmand², R. Chtourou¹ and V. Darakchieva³

We study the effect of nitrogen on the GaAs_{0.9-x}N_xSb_{0.1} ($x = 0.00, 0.65, 1.06, 1.45$ and 1.90 %) alloy dielectric function by spectroscopic ellipsometry in the energy range from 0.73 to 4.75 eV. The compositional dependences of the critical points energies for the GaAs_{0.9-x}N_xSb_{0.1} are obtained. In addition to the GaAs intrinsic transitions E_1 , $E_1+\Delta_1$, and E_0' , the nitrogen-induced Γ -point optical transitions E_0 and E_+ , together with a third transition $E^\#$, are identified. We find that with increasing the N content, the E_0 transition shifts to lower energies while the E_+ and $E^\#$ transitions shift to higher energies. We suggest that the origin of the E_0 , E_+ and $E^\#$ transitions may be explained by the double band anticrossing (BAC) model, consisting of a conduction BAC model and a valence BAC model.

¹ Laboratoire de Photovoltaïque de Semiconducteurs et de Nanostructures, Centre de Recherche et de Technologie de l'Énergie, BP. 95, Hammam-Lif 2050, Tunisia.

² Laboratoire de Photonique et de Nanostructures, CNRS Route de Nozay, 91 460, Marcoussis, France.

³ Department of Physics, Chemistry and Biology, Linköping University, SE-581 83 Linköping, Sweden.

Optical properties of InN/In_{0.73}Ga_{0.27}N multiple quantum wells studied by spectroscopic ellipsometry

N. Ben Sadrine,¹ V. Darakchieva,² D. Lindgren,² B. Monemar,² S.B. Che,² Y. Ishitani,³ A. Yoshikawa³

The optical properties of two high quality fifty-periods of In-polarity InN/In_{0.73}Ga_{0.27}N MQWs samples, grown by radio-frequency plasma-assisted molecular beam epitaxy, with different well (0.5-1nm) and barrier thicknesses (3-4nm) were studied. We employ spectroscopic ellipsometry at room temperature in the energy range from 0.6 to 6 eV, and incidence angles of 60 and 70°. Ellipsometric data were successfully modelled using the model dielectric function approach and a multilayer model assuming the MQWs as a homogeneous layer. The E₀, A and E₁ MQWs transition energies were determined and found to exhibit a blueshift with decreasing the well thickness.

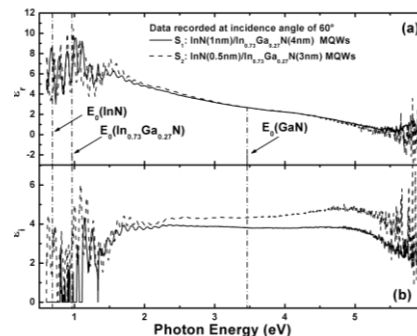


Fig. Pseudodielectric function real and imaginary parts for both samples.

¹ Laboratoire de Photovoltaïque de Semiconducteurs et de Nanostructures, Centre de Recherche et de Technologie de l'Énergie, Tunisia.

² Department of Physics, Chemistry and Biology, Linköping University, SE-581 83 Linköping, Sweden.

³ Graduate School of Electrical and Electronic Engineering, Chiba University, 263-8522 Chiba, Japan.

Optical active centres in ZnO samples

T. Monteiro¹, M.J. Soares¹, A. Neves¹, S. Pereira¹, M.R. Correia¹, M. Peres¹, E. Alves, D. Rogers², F. Teherani², V. Munoz-SanJose³, T. Trindade⁴ and A. Pereira⁴

ZnO ($E_g \approx 3.37$ eV) is an semiconductor oxide with enhanced properties for a wide range of opto-emitter applications spanning visible and short wavelengths. Bulk, thin films and nanomaterials obtained using different synthesis methods have been investigated for optoelectronic and biotechnological device applications. Nominally undoped bulk samples typically present a myriad-structured near-band-edge recombination, mainly due to free/bound excitons and donor–acceptor pair transitions. Furthermore, deep level emission due to intrinsic defects and extrinsic impurities, such as transition metal ions, are commonly observed in different grades of bulk ZnO samples. Undoped thin film and ZnO nanocrystal samples also present optically-active centres due to the presence of native and extrinsic defects. Continuing improvement in device performance hinges on improved understanding of the role of these defects present in ZnO samples. In this work a correlation between the optical centres was observed between nominally-undoped bulk, thin films and nanocrystal ZnO. We also observed a correlation between the structural properties and ion optical activation for single crystal samples which were intentionally-doped with rare earth ions (Tm, Er, Eu and Tb) either (a) by ion-implantation or (b) during synthesis. For the doped ZnO nanocrystals, intra-ionic recombination and XRD data suggest that the ions are in a crystalline environment.

¹ Departamento de Física, Universidade de Aveiro, 3810-193 Aveiro, Portugal.

² Nanovation, Orsay 91400, France.

³ Departamento de Física Aplicada, Universidad València, València, Spain.

⁴ Departamento de Química, CICECO, Universidade de Aveiro, 3810-193 Aveiro, Portugal.

Mn-doped ZnO nanocrystals embedded in Al₂O₃: structural and electrical properties

A Khodorov¹, S Levichev¹, A G Rolo¹, O Karzazi², A Chahboun^{1,2}, J Novak³, A Vorobiev³, C J Tavares¹, D Eyidi⁴, J-P Rivièrè⁴, M F Beaufort⁴, N P Barradas, E Alves, L.C. Alves, D J Barber⁵, S Lanceros-Mendez¹, M J M Gomes¹

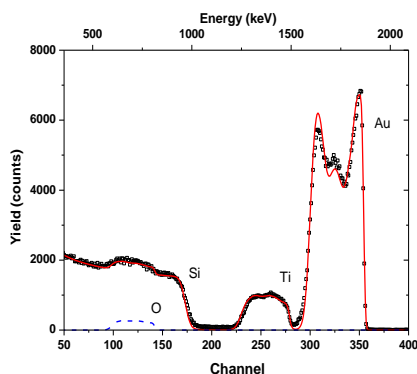
The structural and electrical properties of Mn-doped ZnO/Al₂O₃ nanostructures produced by the pulsed laser deposition technique were studied by grazing incidence small angle x-ray scattering (GISAXS), Rutherford backscattering spectrometry and capacitance–voltage measurements. The results revealed the multilayered structure in as-deposited samples and the annealing of the nanostructures at high temperatures was shown to promote the formation of nanocrystals embedded in the Al₂O₃ matrix, as was evidenced by GISAXS and high resolution transmission microscopy. Particle-induced x-ray emission analysis showed a doping of 8 at.% Mn in ZnO. Grazing incidence x-ray diffraction and Raman spectroscopy demonstrated that the nanocrystals have the pure wurtzite ZnMnO crystalline phase. Resonant Raman scattering displayed an increase of intensity of the 1LO mode as well as broadening of the 2LO mode related to the size effect. Capacitance–voltage measurements showed carrier retention with a voltage shift higher than those reported for similar systems.

¹ Centre of Physics and Physics Department, University of Minho, 4710-057 Braga, Portugal; ² LPS, Physics Department, Faculty of Sciences, Fès, Morocco; ³ ESRF, Grenoble, France; ⁴ PhyMat, University of Poitiers, 86962 Futuroscope-Chasseneuil, France ; ⁵ Physics Centre, University of Essex, Colchester, CO4 3SQ, UK.

Functional and optical properties of Au:TiO₂ nanocomposite films: The influence of thermal annealing

M. Torrell¹, L. Cunha¹, A. Cavaleiro², E. Alves, N.P. Barradas and F. Vaz¹

A set of nanocomposite thin films consisting of Au nanoclusters dispersed in a TiO₂ dielectric matrix was deposited by reactive magnetron sputtering, and subjected to thermal annealing in vacuum, at temperatures ranging from 200 to 800 °C. The obtained results show that the structure and the size of Au clusters, together with the matrix crystallinity, changed as a result of the annealing, and were shown to be able to change the optical properties of the films and keeping good mechanical properties, opening thus a wide number of possible applications. The crystallization of the gold nanoclusters induced by the annealing was followed by a systematic change in the overall coating behaviour, namely the appearance of surface plasmon resonance (SPR) behaviour. This effect enables to tailor the thin films reflectivity, absorbance and colour coordinates, contributing to the importance of this thin film system. The different attained optical characteristics associated with a reasonable mechanical resistance of the coatings induce the possibility to use this film system in a wide range of decorative applications.



¹ Universidade do Minho, Dept. Física, Campus de Azurém, 4800-058 Guimarães, Portugal.

² SEC-CEMUC–Universidade de Coimbra, Dept. Eng. Mecânica, Pólo II, 3030-788 Coimbra, Portugal.

Effects of Mg-ion implantation in α-Al₂O₃ and α-Al₂O₃:Mg crystals: Electrical conductivity and electronic structure changes

M. Tardío¹, I. Colera¹, R. Ramírez¹ and E. Alves

Undoped and Mg-doped α-Al₂O₃ single crystals were implanted with Mg ions, with an energy of 90 keV and a fluence of 10¹⁷ ions/cm². DC electrical measurements using the four-point probe method, between 295 and 428 K, were used to characterize the electrical conductivity of the implanted area. Measurements in this temperature range indicate that the electrical conductivity after implantation is thermally activated with an activation energy of about 0.03 eV both in undoped and in reduced Mg-doped α-Al₂O₃ crystals, whereas the activation energy in oxidized Mg-doped α-Al₂O₃ crystals remains close to that before implantation. The I–V characteristics of the latter samples reveal a blocking behavior of the electrical contacts on the implanted area in contrast to the ohmic contacts observed in α-Al₂O₃ single crystals with the c-axis perpendicular to the broad face, where the Mg ions were implanted. We conclude that the enhancement in conductivity observed in the implanted regions is related to the intrinsic defects created by the implantation, rather than to the implanted Mg ions. The relationship between the oxygen vacancy concentrations at different stages of etching and the changes in the electronic structure, the chemical bonding, and the Al³⁺(2p)/O²⁻(1s) and Mg²⁺(1s)/O²⁻(1s) relative intensities was studied by X-ray Photoemission Spectroscopy.

¹Universidad Carlos III de Madrid, Departamento de Física, 28911 Leganés, Madrid, Spain.

Damage recovery and optical activity in europium implanted wide gap oxides

E. Alves, C. Marques, N. Franco, L.C. Alves, M. Peres¹, M.J. Soares¹ and T. Monteiro¹

Defects play an important role on the optical behaviour of sapphire and magnesium oxide single crystals. We studied the optical properties of these oxides implanted at room temperature with different fluences (1 × 10¹⁵–1 × 10¹⁶ cm⁻²) of europium ions. Rutherford backscattering channelling shows that for fluences above 5 × 10¹⁵ cm⁻² the surface disorder level in the Al-sublattice reaches the random level. Implantation damage recovers fast for annealing in oxidizing atmosphere but even for the highest fluence we recover almost completely all the damage after annealing at 1300 °C, independently of the annealing environment (reducing or oxidizing). Annealing above 1000 °C promotes the formation of Eu₂O₃ in the samples with higher concentration of Eu. The optical activation of the rare earth ions at room temperature was observed after annealing at 800 °C by photoluminescence and ionoluminescence. In Al₂O₃ lattice the highest intensity line of the Eu³⁺ ions corresponds to the forced electric dipole ⁵D₀ → ⁷F₂ transition that occurs ≈ 616 nm. For the MgO samples the Eu³⁺ optical activation was also achieved after implantation with different fluences. Here, the lanthanide recombination is dominated by the magnetic dipole ⁵D₀ → ⁷F₁ transition near by 590 nm commonly observed for samples where Eu³⁺ is placed in a high symmetry local site. The results clearly demonstrate the possibility to get Eu incorporated in optical active regular lattice sites in wide gap oxides.

¹ Departamento de Física e I3N, Universidade de Aveiro, 3810-193 Aveiro, Portugal.

Magnetic and transport properties of ZnO single crystals doped by ion implantationC. Silva¹, A.R.G. Costa¹, R.P. Borges¹, M.M. Cruz¹, M. Godinho¹, R.C. da Silva

This research continued on two fronts, implantation doping with *i*) transition metals, and *ii*) non-magnetic gases.

i) Magnetic and transport properties of transition metals doped ZnO

Zinc oxide single crystals were implanted with Mn, Co and Ni ions with 200 keV energy and fluences between $1 \times 10^{16} \text{ cm}^{-2}$ and $1 \times 10^{17} \text{ cm}^{-2}$, and analysed by RBS, RBS/channelling and XRD. Results showed that formation of nm sized particles occurred only in the case of $1 \times 10^{17} \text{ cm}^{-2}$ Ni. The nm sized Ni aggregates display super-paramagnetic behaviour, grow by annealing at 1073 K and oxidize: super-paramagnetism is retained in the oxidized state, but with lower T_B , indicating partial oxidation of Ni and formation of Ni/NiO core shell particles. On the contrary, with Mn super-paramagnetic behaviour was observed only upon 1073 K annealing of the highest implantation fluence, $1 \times 10^{17} \text{ cm}^{-2}$. However, this was assigned to formation of ZnMn_2O_4 nanoparticles rather than Mn aggregation, as detected by XRD, consistently with a general dilution trend of Mn ions upon annealing. In the remaining cases – 1, 2 and $5 \times 10^{17} \text{ cm}^{-2}$ Ni and all but the lowest fluence of Co – annealing at 1073 K lead to aggregate formation and super-paramagnetic behaviour. Correlation with RBS/channelling measurements indicates that this is possibly driven by the dynamics of the annealing induced recovery of crystalline order. Damage and damage recovery as seen by RBS/channelling also correlate with the transport properties, as all the samples are insulating in the as implanted state and acquire measurable conductivities by annealing.

ii) Magnetic and transport properties of nitrogen and argon doped ZnO

Argon and nitrogen ions were implanted into ZnO single crystals with 200 keV energy and fluences of $1 \times 10^{17} \text{ cm}^{-2}$ and $2 \times 10^{17} \text{ cm}^{-2}$ in order to compare the influence of these non-magnetic elements in the magnetic and electrical behaviour of zinc oxide. RBS/channelling measurements showed that the high levels of disorder left in the implanted region are partially annealed only at and above 1073 K. As PIXE measurements show that there are no magnetic elements in the implanted samples, the ferromagnetic behaviour found by magnetic characterization of the as-implanted state, is certainly correlated with the implantation defects in the lattice. After annealing the ferromagnetic components decrease or completely disappear, in consistency with the defect origin of the recorded behaviour.

¹ Dep. Física da Universidade de Lisboa.

Single and polycrystalline mullite fibres grown by laser floating zone techniqueR.G. Carvalho¹, A.J.S. Fernandes¹, F.J. Oliveira², E. Alves, N. Franco, C. Louro³, R.F. Silva² and F.M. Costa¹

The laser floating zone technique was used to grow large $2\text{Al}_2\text{O}_3\text{-SiO}_2$ mullite fibres (up to 1.6 mm in diameter and 40 mm in length). The fibres grown at 10 mm/h are single crystalline in nature, while those pulled at higher rates (40 and 100 mm/h) are polycrystalline with a cellular microstructure. The crystals are highly [0 0 1] textured with respect to the fibre axis, as determined by X-ray diffraction analysis. The Raman spectra taken at different orientations corroborate the strong anisotropy observed by X-ray and SEM on both single crystalline and textured polycrystalline samples. Four point bending tests and ultramicroindentation Vickers experiments were performed at room temperature in order to characterize the mechanical properties. The presence of lamellar inclusions in the single crystalline fibres decreases the flexural strength (431 MPa) and the fracture toughness ($1.2 \text{ MPa}\cdot\text{m}^{1/2}$) compared to the polycrystalline ones (631 MPa and $1.6 \text{ MPa}\cdot\text{m}^{1/2}$). However, the absence of grain boundaries in the single crystals leads to higher ultramicrohardness ($H_V = 15.6 \text{ GPa}$) and Young's modulus ($E = 170 \text{ GPa}$) than those of the polycrystalline fibres (14.2 and 145 GPa), where a glassy intergranular phase exists.

¹ I3N, Physics Department, University of Aveiro, 3810-193 Aveiro, Portugal.

² CICECO, Glass and Ceramic Engineering Department, University of Aveiro, 3810-193 Aveiro, Portugal.

³ CEMUC, Mechanical Engineering Department, University of Coimbra, 3030-788 Coimbra, Portugal.

Transition metals nitrides for magnetic applicationsR.C. da Silva, A.R.G. Costa¹, M.M. Cruz¹, M. Godinho¹

New research has been started in transition metals nitrides aiming at magnetic applications.

Synthesis of Fe, Co and Ni nitrides at the nm scale for magnetic applications has been achieved in various forms, thin films deposited by RPLAD, powders by nitridation of metal oxide particles, and embedded nitride particles made by N ion implantation. Deposition parameters of the thin films were studied, RBS analysis showing that in *e.g.* Co-nitride a stoichiometric layer is readily obtained from a low pressure pure N_2 atmosphere. As for the implanted metals, RBS and XRD measurements showed that N ions were successfully retained to fluences of $1\text{-}2 \times 10^{17} \text{ cm}^{-2}$ and that nitrides did form in Fe and Ni – as Fe_2N and Ni_3N – but not in Co.

¹ Dep. Física da Universidade de Lisboa.

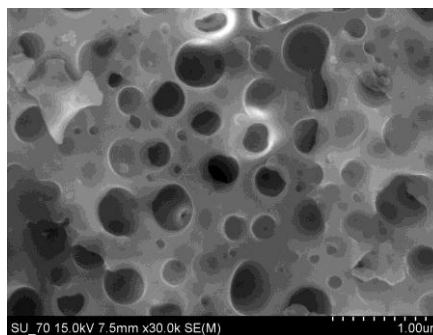
Stoichiometry changes of BFO in the thin film formR.C. da Silva, B. Ribeiro¹, R.P. Borges¹

A number of BaFe_{1-x}O₃ thin films (BFO) of thicknesses in the range 50 nm to 120 nm were deposited onto SrTiO₃ (STO) substrates and its compositions analysed by RBS in order to ascertain the cations ratios [Ba]:[Fe]. Detailed analysis was performed by assigning initial compositions and thicknesses for the films and allowing the RUMP[®] code to simulate the expected RBS spectra. In each case the theoretically simulated spectrum was compared with the corresponding experimental spectrum and the compositions reworked to reach convergence. By using the PERT module of the RUMP[®] package the layers compositions and/or thicknesses were left free to be varied over intervals from ±5% up to of as much as ±20% of the nominal values, in a fitting procedure by a non-linear least squares method. From these analyses a number of conclusions are extracted:

- The cation compositions are slightly Ba-rich, with an average [Fe]:[Ba] smaller than but close to unity;
- The overall compositions are O-rich (*i.e.* cation deficient) in relation with the nominal composition, with an anion to cation ratio above 1.5 by less than 5%.

¹ Dep. Física da Universidade de Lisboa.**Structural and thermal characterization of SiO₂-P₂O₅ sol-gel powders upon annealing at high temperatures**M. Elisa¹, B.A. Sava², A. Volceanov³, R.C.C. Monteiro⁴, E. Alves, N. Franco, F.A. Costa Oliveira⁵, H. Fernandes⁶ and M.C. Ferro⁶

This study deals with SiO₂-P₂O₅ powders obtained by sol-gel process, starting from tetraethoxysilane (TEOS) as precursor for SiO₂ and either triethylphosphate (TEP) or phosphoric acid (H₃PO₄) as precursors for P₂O₅. In the case of samples prepared with H₃PO₄, TG-DTA data showed an accentuated weight loss associated to an endothermic effect up to about 140 °C, specific for the evaporation of water and ethylic alcohol from structural pores, and also due to alkylamines evaporation. Sol-gel samples prepared with TEP exhibited different thermal effects, depending on the type of atmosphere used in the experiments, *i.e.* argon or air. XRD analysis revealed that annealed sol-gel samples prepared with H₃PO₄ showed specific peaks for silicophosphate compounds such as Si₃(PO₄)₄, Si₂P₂O₉, and SiP₂O₇. XRD results for annealed sol-gel samples prepared with TEP indicated mainly the presence of a vitreous (amorphous) phase, which could be correlated with SEM images. The presence of SiO₂ in the sample might be expected. Thus, we have searched for any SiO₂ polymorph possible to crystallize. Only potential peaks of cristobalite were identified but some of them are overlapping with peaks of other crystalline phosphates. SEM analysis indicated a decrease of the amount of crystalline phases with the increase in the annealing temperature.

¹ National Institute of Optoelectronics-INOE 2000, 1, Atomistilor Str., P.O. Box MG-5, 77125, Bucharest-Magurele, Romania.² National Institute of Glass S.A., 47th Pallady Bvd, Bucharest 032258, Romania.³ Politehnica University of Bucharest, Faculty of Applied Chemistry and Materials Science, P.O. Box 12-134, Bucharest, Romania.⁴ New University of Lisbon, Department of Materials Sciences, CENIMAT/13N, 2829-516 Caparica, Portugal.⁵ Laboratório Nacional de Energia e Geologia I.P., Product Engineering Unit, Estrada de Paço de Lumiar-1649-038, Lisboa, Portugal.⁶ University of Aveiro, University Campus of Santiago, 3810-193 Aveiro, Portugal.**Study of double layer metal contacts on CdZnTe for radiation detectors.**Q. Zheng¹, F. Dierre¹, R. Fernández-Ruiz², V. Corregidor, J. Crocco¹, H. Bensalah¹, E. Alves, E. Diéguez¹

Cd(Zn)Te is a II-VI semiconductor with a wide range of room temperature nuclear applications, used for medical, industrial and safety systems. To take in advantage the electronic properties of the Cd(Zn)Te, ohmic contacts are classically deposited to obtain detectors with low leakage current, extended electrical field profile and higher detector efficiency. Nanometric double layers of different metal-semiconductor-metal (MSM) depositions on CdZnTe substrates were deposited at Crystal Growth Laboratory (Madrid) by electroless method. At ITN, RBS was used to determine the thickness, depth profiles and the composition of the layers deposited at the surface. The results have contributed to a better knowledge of the mechanisms involved during the deposition, where the Cd ions are rejected into the solution and tellurium oxide is incorporated during the contacts growth. Among the different metals used (Pt, Ru, Rh, Au, Pd), Pt contacts have shown a linear ohmic behaviour and a good gamma response by ⁵⁷Co source. On the other hand, Ru and Rh contacts have a poor gamma response, indicating that the process have to be optimized.

¹ CGL, Physics Department, Autónoma University of Madrid, Spain.² SiDI, Autónoma University of Madrid, Spain.

Study of alternative substrates for the deposition of Si nanowires

A.Kling, A. Rodríguez¹, T.Rodríguez¹

Although the first synthesis of Si nanowires dates back to 1957 interest in them revived recently due to their unique physical properties, e.g. light emission, field emission, and quantum confinement effects. Among the various known methods for the production of Si nanowires chemical vapor deposition using Au-coated Si substrates is one of the most frequently used where the gold acts as a catalyst. Despite its innumerable advantages gold is not compatible with present state CMOS technology production standards and therefore alternative catalyst materials are procured. Sn and Au-Ga alloy layers were deposited on Si wafers and their thickness and composition studied by RBS using 2 MeV He⁺ ions for as-deposited and annealed samples. It was found that in the case of Sn even at room temperature oxidation occurs that affects also the underlying Si. On the other hand, Au-Ga alloys show only a minimal oxidation on the surface but react strongly with the silicon during annealing at 500°C. He-RBS spectra could only be fit assuming a small but in the spectra virtually invisible carbon contamination of the Au-Ga alloy. Additional studies using the strong ¹²C(p,p)¹²C scattering resonance at about 1.75 MeV were performed to corroborate the presence of carbon and quantify it. The origin of this contamination is presently under investigation.

¹ Dpto. Tecnología Electrónica, E.T.S.I. de Telecomunicación, Universidad Politécnica de Madrid, 28040 Madrid, Spain.

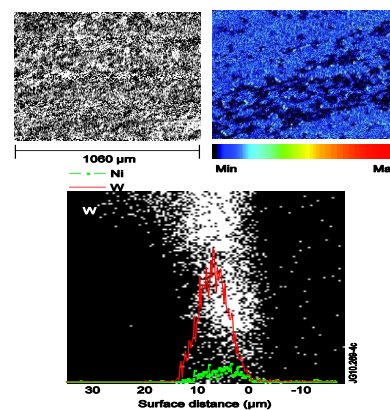
Surface composition and morphology changes of materials for fusion reactors

L.C. Alves, E. Alves, N P Barradas, R. Mateus¹, P. Carvalho¹, J.P.Coad², A. M. Widdowson², J. Likonen³, S. Koivuranta³, V. Chakin⁴, A. Moeslang⁴, P. Kurinsky⁴, R. Rolli⁴, H.-C. Schneider⁴, JET-EFDA Contributors#

The use of ion beams for the study of materials for fusion reactors has been centered in the characterization of: i) - Beryllium pebbles and V/Ti beryllides degree and extent of oxidized surface layer after air annealing at temperatures of 600 °C, 800 °C and 1100 °C; ii) - Erosion and redeposition processes at the JET first-wall carbon tiles during plasma operations;

i) The beryllium pebbles annealed at 600 °C and 800 °C present an oxidized layer extending from 0.15 μm up to 0.25 μm. At 1100 °C, some of the pebbles have a strong oxidation reaction leading to the alteration of surface morphology and even to the detachment of Be oxide. In what concerns beryllides, the formed oxide layer after air annealing at 800 °C during 1 h, is larger in the case of the V beryllide (~0.7 μm) than for the Ti beryllide (~0.3 μm).

ii) Marker tiles containing a thin W layer were mounted in the JET vessel in order to study erosion-deposition processes in different areas of the reaction chamber during JET plasma operations. Broad and microbeam ion techniques allowed determining surface and/or depth profile distribution of several elements such as W (the used marker) Ni, Cr, Fe (Inconel structural material) and Be (plasma impurity), contributing for predicting the lifetime of components for future devices such as ITER. Still related with fusion materials, the study of surface alterations of beryllium pebbles and V/Ti beryllides under high-fluence neutron irradiation is being carried out.



¹ EURATOM/IST Portugal; ² EURATOM/CCFE UK; ³ EURATOM/TEKES Finland, ⁴ KIT Germany.

Hydrogen retention in gallium samples exposed to ISTTOK plasmas

R.B. Gomes¹, R. Mateus¹, E. Alves, H. Fernandes¹, C. Silva¹, P. Duarte¹

The use of liquid metals such as lithium and gallium have been pointed out as a suitable solution to solve problems related to the use of solid walls submitted to high power loads. A proper use of liquid materials in fusion reactors depends on their affinity to retain hydrogenic isotopes. While retention in lithium has been studied in detail, less is known for gallium. Taking into account the deep influence of this property on plasma behavior it is deemed relevant to perform such studies in tokamak plasmas. An experimental setup has been developed to produce high purity gallium samples which were exposed to ISTTOK plasmas on both liquid and solid phases. Hydrogen retention and in-depth profiles were simultaneously measured by ERDA and RBS analytical techniques. Experimental data proved that most of the retention takes place in a thin layer near the surface. Liquid samples present higher retention values which may be understood if higher hydrogen diffusivity is assumed. Retained fraction ($H_{retained}/H_{incident}$) around 0.3 and 1 % were obtained for solid and liquid samples, respectively.

¹ Instituto de Plasmas e Fusão Nuclear, Instituto Superior Técnico, 1049-001 Lisboa, Portugal.

Carbon deposition on beryllium substrates and subsequent delamination

R. Mateus¹, N. Franco, L.C. Alves, M. Fonseca², P.A. Carvalho^{1,3}, E. Alves

Beryllium and carbon are foreseen as materials for plasma facing components of future fusion devices. Erosion, re-deposition and annealing arising from heat-load events during reactor operation will produce mixed material layers and compounds on the plasma facing surfaces, leading to changes in local melting point, sputtering behaviour, hydrogenic species retention and dust formation due to delamination.

In order to mimic the erosion/deposition processes, carbon layers have been evaporated onto beryllium plates and annealed in the 373 to 1073 K range for 90 min. Ion beam measurements revealed a smooth beryllium and carbon interdiffusion at the samples surface up to 773 K. A carbide formation reaction front became apparent for higher temperatures in scanning electron microscopy observations, with the volume fraction of Be₂C crystals resulting also evident in X-ray diffraction patterns. The annealing treatments induced delamination of large surface areas through telephone cords blistering attributed to strain energy release. At 1073 K cracking occurred preferentially along blister boundaries. This fracture behaviour seems caused by the different thermal expansion coefficients of the phases. The results show that delamination of re-deposited layers in PFCs is a natural mechanism of dust formation.

¹ Instituto de Plasmas e Fusão Nuclear, Instituto Superior Técnico, 1049-001 Lisboa, Portugal.

² Centro de Física Nuclear, Universidade de Lisboa, 1649-003 Lisboa, Portugal.

³ ICEMS, Departamento de Engenharia de Materiais, Instituto Superior Técnico, 1049-001 Lisboa, Portugal.

Ni-Ti alloy surface modified by plasma immersion ion implantation of nitrogen

R.M.S. Martins, N. Barradas, E. Alves, D. Henke¹, H. Reuther¹, J.C.S. Fernandes²

The wide spectrum of applications in implantology imposes special requirements on the biocompatibility of Ni-Ti. The use of coatings in order to modify the surface characteristics of a material is a widely used approach. However, in the case of medical devices whose shape or size is modified during the procedure of insertion or due to the working conditions, metallic or metal oxide coatings may crack. In the frame of project SPIRIT-77, plasma-immersion ion implantation (PIII) has been employed in order to overcome these limitations. This technique was used to modify and improve the superficial region of a superelastic (at body temperature) Ni-Ti alloy. The working plan comprised ion implantation of nitrogen. The experiments were performed in a HV chamber, with a base pressure of 3×10⁻⁴ Pa and a working pressure of 0.2 Pa, equipped with an RF plasma source operating at a power of 350 W. High voltage pulses of either 20 or 40 kV and length of 5 μs were applied to the samples using a frequency of 400 Hz. The sample holder was not intentional heated (T < 125°C). The depth profiles of the elemental distribution in the alloy surface region, obtained by Auger electron spectroscopy, clearly show a Ni-depleted fraction for experiments performed with 40 keV (Figure 1) due to the formation of titanium oxynitride (TiN_xO_y). Furthermore, the PIII technique leads to a graded interface between the modified surface and the bulk Ni-Ti alloy, which is a plus for improving adhesion.

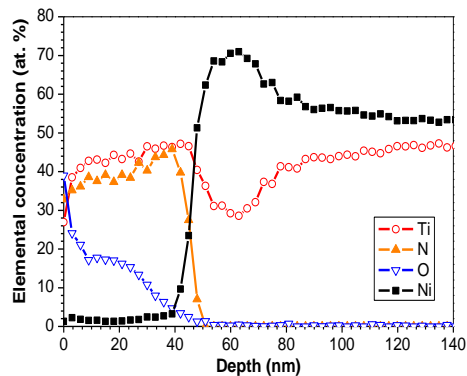


Figure 1: Results obtained for a Ni-Ti sample implanted with nitrogen (40 keV; 1 hour).

¹ Institute of Ion Beam Physics & Materials Research, Forschungszentrum Dresden-Rossendorf, P.O.Box 510119, 01314 Dresden, Germany.

² ICEMS/DEQB, Instituto Superior Técnico, TULisbon, 1049-001 Lisboa, Portugal.

Corrosion in XV and XVI century stained glasses

M. Vilarigues^{1,2}, A. Ruivo^{2,3}, P. Redol^{1,4}, A. Machado¹, P.A. Rodrigues¹, V. Corregidor, L.C. Alves, R.C. da Silva

The study of corrosion in two stained glass panels from the south aisle of St^a. Maria da Vitória Monastery, at Batalha (Portugal), was also carried out. These panels exhibit extensive corrosion with darkening phenomena. By using external μPIXE and μPIGE, the elemental compositions of large fragments were obtained, enabling the selection of representative corroded areas, from which elemental distribution maps were produced. Calcium and potassium rich structures were found – at the surface and inside cavities in the glass – that were identified as oxalates and carbonates, by Raman microscopy and μFTIR. The dark spots in the glass surfaces were found to be Zn and Pb rich. These findings indicate that the corrosion observed was due not only to reactions with atmospheric water and CO₂ but also with the oxalic acid secreted by micro-organisms. Furthermore, it did not result from reactions with atmospheric SO₂ or acid rain.

¹ DCR/FCT-UNL; ² VICARTE/FCT-UNL; ³ REQUINTE/FCT-UNL; ⁴ Mosteiro da Batalha.

Medieval Yellow silver staining – Convento de Cristo, Tomar

M. Vilarigues^{1,2}, J. Delgado¹, A. Ruivo^{2,3}, H. Marçal¹, V. Corregidor, L.C. Alves, R.C. da Silva

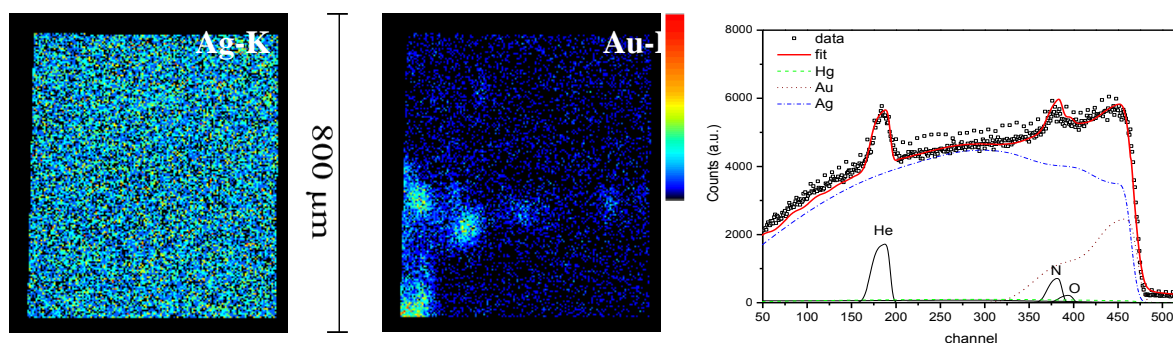
The technique of yellow silver staining consists on applying a diluted Ag salt at the glass surface which is then fired at temperatures between 500 °C and 650 °C. However, the yellow silver stained glass fragments recently discovered in Convento de Cristo, contain an Ag-Cu mixture. In order to understand the role of Cu and the influence of the firing temperature and glass type on the resulting colours, several soda and potash glasses were produced, stained with Ag or with a Ag-Cu mixtures and characterised using μ XRF, μ PIXE and optical spectroscopy in the UV-Vis range. Three of the fragments display a single absorption band in their UV-Vis spectra, each centred at 418 nm wavelength which is consistent with the formation of a colloidal dispersion of spherical Ag nanoparticles with dimensions of \sim 10 nm. The fragments with more vivid colours, on the other hand, present a two band absorption spectra, that may indicate the formation of either non-spherical nanometer-sized particles, or a bimodal distribution of particles sizes. Although the finest yellow colours were observed in the soda laboratory glasses, either stained with Ag or with a Ag-Cu mixture, the ones with Ag-Cu staining were obtained at lower firing temperatures. The role played by Cu in this process could not be attributed to the formation of Cu nanoparticles, since the surface plasmon resonance at \sim 565 nm could not be found in the UV-Vis spectra. For all the laboratory samples stained with a Ag-Cu compound mixture or in the historical fragments, the corresponding concentration depth profiles obtained by μ PIXE show that Ag penetrates into the glass during the annealing, leaving Cu behind and closer to the surface. It can also be noticed that the Ag diffusion extent on these laboratory glasses is significantly smaller than the one observed when only the Ag solution is used. The obtained experimental results can be understood consistently, if the transit time, i.e. the time available for atom-metal cluster interaction by diffusion, is the key parameter for the growth of the Ag nanoparticles and their final dimensions at a given firing temperature. Cu seems to play an important role in the increment of the transit time.

¹ DCR/FCT-UNL; ² VICARTE/FCT-UNL; ³ REQUINTE/FCT-UNL.

Characterization of Mercury Gilding Art Objects by External Proton Beam

V. Corregidor, L.C. Alves, N.P. Barradas, M.A. Reis, M.T. Marques^{1,2}, J.A. Ribeiro^{1,2}

The fire gilding is one of the methods used by the ancient goldsmiths to obtain a rich, metallic glow and durable golden appearance in ornamental objects. This layer is characterized, among others, by its thickness (several microns) a diffusion profile and a Hg content (between 0–21 wt%) depending on the temperatures achieved during the process. Gilded sacred art objects dated from the XVI to the XVIII centuries, belonging to the Casa-Museu Dr. Anastácio Gonçalves Collection (Lisbon) were analysed using the external ion microprobe at Nuclear and Technological Institute, Lisbon. The average concentrations of homogeneous areas were calculated with GUPIX, DATPIXE and NDF codes showing very similar results. Efforts related with finer detector efficiency calibration, stability of the He flow control and data base consistency issues should be done to overcome the registered differences. Generally speaking, and comparing the composition extracted for several points on two of the pieces which are totally gilded, the ostensorium, from the mid-XVIII century, has an average Hg content (12 %) which is larger than the one observed for the reliquary, from the XVI century, (10 %). About two centuries separate the goldsmiths responsible for these objects and probably different production locations and sources of the materials explain the differences between them. In some particular cases the simultaneous fitting of the RBS and the PIXE experimental data reveals that the inhomogeneous composition observed in the PIXE maps are mainly due to superficial inclusions which are Au rich with a diffusion profile into the silver object. (Figure 1)



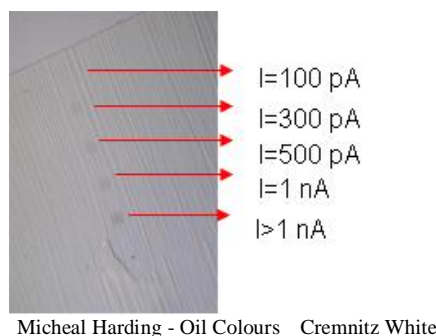
¹ Casa-Museu Anastácio Gonçalves, Av. 5 de Outubro, 6-8 1050-055 Lisboa, Portugal.

² IMC, Palácio Nacional da Ajuda, 1349 – 021 Lisboa, Portugal.

Induced defects by an external proton beam on pigments used on easel paintings

V. Corregidor, L.C. Alves, N.P. Barradas, M.A. Reis

IBA techniques using an external proton beam can be applied to Cultural Heritage objects, giving information about the elemental composition of a punctual or a determined area. One of the applications is the easel paintings, to determine the composition of the pigments used by the painters. In some cases, this information can help to assign the painter, date the paint or discover later conservation process. Although the techniques are considered as non-destructives, in some cases some defects can be created if carbonate minerals are involved, with the appearance of dark brownish regions that eventually disappear along the time. To avoid the presence of this induced defects, the experimental conditions (beam current, time of measurement, etc.) should be optimized. In this work white colours from Michael Harding chart colour were analysed as a function of beam current, varying from 0.1 nA to 1.5 nA. On the “Titanium White N.2”, made of zinc oxide and titanium oxide, weak visible marks were observed after the measurements when higher currents were used but they disappear after few hours. On the other hand, the “Cremnitz White”, made of lead carbonate, visible marks were detected even using low current values (figure 1). The marks fade out along the weeks, and after five months the marks made using the higher current values are still visible. Efforts should be done to reduce the marks, not only optimizing the experimental conditions but also the post-treatments to accelerate the fade out process. These treatments have to guarantee the integrity of the art objects, so no heat treatments or aggressive one should be considered.



Synchrotron-radiation based micro-computed tomography applied to the characterization of dinosaur eggshells

Rui M.S. Martins¹, Octávio Mateus^{1,2}, Felix Beckmann³, Philipp Klaus Pranzas³

The study of fossilized eggshells is a very important topic for the Museum of Lourinhã. Although the eggshell fragments are subject to diagenetic processes unique features can be preserved. The histology of the eggshell provides information with biological and paleoenvironmental implications. For example, the eggshell pore pattern is associated with gas exchange ratios between nest environment and embryo. Therefore, the study of the porosity of the shell can provide valuable information about the level of humidity of the area where the egg was laid. The synchrotron radiation based micro-computed tomography (SR μ CT) studies have been performed at the beamline HARWI II at the storage ring DORIS III located at DESY in Hamburg, Germany. The eggshell fragments have been collected in three different sites of the Lourinhã formation, namely: Peralta, Paimogo and Porto de Barcas (Figure 1a). The first data recorded for eggshells is shown in the figure below. The effective pixel size corresponds to 6.4 μ m, which allows a direct, non-destructive visualization of the morphology of the pores and their connectivity in the eggshell fragments, providing information that is either exceedingly difficult or impossible to obtain by traditional methods based on section cutting.

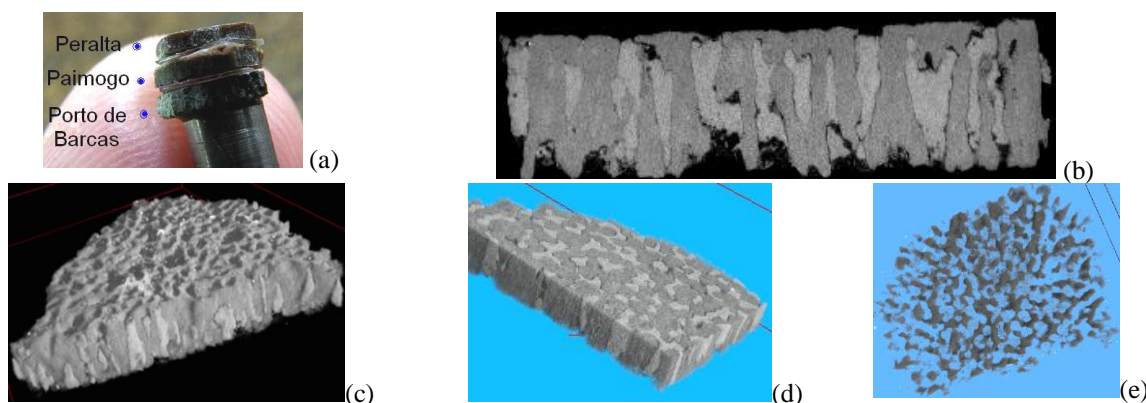


Fig. Eggshell fragments collected in three different localities of the Lourinhã Formation (Peralta, Paimogo and Porto de Barcas): (a) photograph of the eggshell pieces mounted on the sample holder used for SR μ CT; (b) a microtomographic slice through the eggshell type of the locality of Porto de Barcas; (c) a three-dimensional image of the complete sample of the locality of Porto de Barcas; (d) sectioning of the three-dimensional image of the sample of figure 1c providing information about pore connectivity in the eggshells; (e) pore canals run through the shell which permit gas exchange between the embryo and atmosphere.

¹ Museu da Lourinhã, Rua João Luis de Moura, 2530-157 Lourinhã, Portugal.

² CICEGe, Faculdade de Ciências e Tecnologia, FCT, Universidade Nova de Lisboa, 2829-516 Caparica, Portugal.

³ Helmholtz-Zentrum Geesthacht, Institute of Materials Research, Max-Planck-Str. 1, 21502 Geesthacht, Germany.

Study of dinosaur eggshells from the Lourinhã Formation by x-ray diffractionRui M. S. Martins¹, Norbert Schell²

X-ray powder diffraction has proven itself to be a valuable tool in geochemistry and mineralogy. However, although this technique can be useful to determine if eggshells had undergone diagenetic alteration, a detailed study of their structure from the external surface to the internal surface is required in order to “map” mineralogical alterations. The eggshell fragments selected for the experiments at the High Energy Materials Science beamline HEMS side station at PETRA III have been collected in two different sites of the Lourinhã Formation, namely: Paimogo and Peralta. The eggshell type detected in Paimogo, of thickness of about 0.92 mm, is ascribed to the theropod *Lourinhanosaurus antunesi*. The external morphology and the size of the eggshells of Paimogo and Peralta sites are comparable. They can be from the same species or a closely related taxon. However, more details are required to draw final conclusions. X-ray diffraction data was acquired in transmission mode (image plate MAR345) using a beam spot of 0.1 mm in vertical with 87 keV energy. The measurement carried out at the topmost zone of the eggshell shows that although the main mineral content of the samples was found to be calcite there is also quartz in the sample from Paimogo. The presence of very weak diffraction peaks associated with quartz is still noticeable in the data obtained at the central zone of the eggshell fragment collected at Paimogo site. On the other hand, the intensities of the diffraction peaks related to calcite are quite similar for both samples. It is suggested that in either case, the original shell material was composed of calcite. The internal surface of the shell from Peralta shows as well the presence of quartz and apparently a higher content of this phase is available in this sample zone when compared to the sample from Paimogo. Furthermore, the presence of fluorapatite was identified. This study provides information that helps us to create models about the diagenetic processes. It will be more accurate the comparison between eggshell fragments collected at different sites which is done aiming the identification of species.

¹ Museu da Lourinhã, Rua João Luis de Moura, 2530-157 Lourinhã, Portugal.² Helmholtz-Zentrum Geesthacht, Max-Planck-Str. 1, 21502 Geesthacht, Germany.**Stopping power of ¹¹B in Si and TiO₂ measured with a bulk sample method and Bayesian inference data analysis**Z. Siketić¹, I. Bogdanović Radović¹, E. Alves and N.P. Barradas

The popular stopping power interpolative schemes require experimental data to be developed. Where the data bases are sparse, with few experiments available, interpolations can be more inaccurate. This is the case for the stopping of heavy ions, where even for important targets such as Si there is a need for more measurements. For compounds, the situation is even worse with very few measurements available. In particular, the stopping in oxides and nitrides often deviates significantly from what would be expected using the Bragg's rule. We apply a method that uses bulk or thick film samples to determine the stopping power of ¹¹B in Si and TiO₂. The method, which relies on Bayesian inference analysis of RBS spectra obtained at different energies, has been previously validated by verifying the results obtained in the well-known system ⁴He in Si.

¹ Ruđer Bošković Institute, P.O. Box 180, Zagreb 10002, Croatia.**Data analysis software and Pitfalls in Ion Beam Analysis**N. P. Barradas, C. Jeynes¹, E. Rauhala²

The 2nd Edition of the Handbook of Modern Ion Beam Analysis (IBA) was published in 2010, and included a chapter dedicated to data analysis software for ion beam analysis and another one about the pitfalls of IBA. The data analysis software in ion beam methods are computer programs designed to extract information about the sample from the measured ion beam spectra. The desired information includes identification of sample elements, their concentrations, areal densities and thicknesses of layers. At best, one spectrum can be converted to concentration depth distributions of all elements in the sample. Often, however, such a full description of the sample based on a single experiment is not possible. The analyst can then perform additional experiments with different experimental parameters such as ion energies, different measurement geometry, use another ion beam technique, or include information from other complementary techniques. The chapter deals mainly with the data analysis software of particle-particle ion beam analysis techniques, RBS, ERDA and NRA. Short sections on PIXE and other techniques such as NRP and channelling were also included. The chapter on pitfalls showed how to avoid many problems when determining elemental depth profiles accurately with light-ion Rutherford backscattering spectrometry (RBS) using MeV ion beams. IBA can, of course, use various other beams and related techniques and use these for a variety of other purposes, including profiling of crystalline defects. The discussion presented therefore also covered pitfalls in a number of other important examples

¹ University of Surrey Ion Beam Centre, Guildford, England.² Accelerator Laboratory, University of Helsinki, Finland.

Development and deployment of a micro-tomography system at the ITN nuclear microprobe

A.C. Marques, R.C. da Silva, L.C. Alves

Ion beam tomography offers an essentially non-destructive way of obtaining 3D information at a microscopic level. A new project aiming at developing and deploying a micro-tomography system at the ITN nuclear microprobe started this year. First sets of Scanning Transmission Ion Microscopy (STIM) 2D maps obtained by irradiation under different angles and also of Particle Induced X-ray Emission (PIXE) 2D maps obtained by irradiating at closely spaced energies (and constant angle) successfully served three main purposes: *i*) demonstrating the feasibility of tomographic experiments with the existing equipment, as is, or with only minor changes; *ii*) identifying and solving experimental difficulties, *e.g.* rotational misalignment artefacts, implying new mechanical setup and/or *a posteriori* correction strategies; *iii*) testing and selecting methodologies and programs for manipulation and conversion of 2-D projection maps to tomograms and 3-D image rendering, as well as devising technique-specific issues for reconstruction algorithms to operate on the measured projection data. One difficulty of paramount importance is the lack of accurate rotational positioning of the existing goniometer. This is being solved by design and installation of a more precise and mechanically stable rotation system and a new sample holder fitting to the rotation rod. Sets of synthetic projection maps were generated and successfully used to test and adapt freeware reconstruction software [Tomography, Florida State Univ.]. Using this software, the projection data obtained by STIM was successfully reconstructed with a filtered back projection algorithm (BFP): a test STIM tomography experiment was performed on a butterfly wing by irradiating it with 2 MeV protons at equally spaced tilts, between -60° and $+60^\circ$, yielding a set of 17 projection maps, 256×256 pixels across (corresponding to a scanned area of $1320 \times 1320 \mu\text{m}^2$). A Hamamatsu S1223-01 PIN diode detector was used for data collection, in an off-axis geometry arrangement. The collection times were around 5 minutes per STIM map. The 3-D reconstruction of the scanned wing volume, obtained by means of the BFP algorithm is shown in Fig.1, along with one 2-D projection map as obtained in the STIM experiment. Although only a first test, the reconstruction already reveals

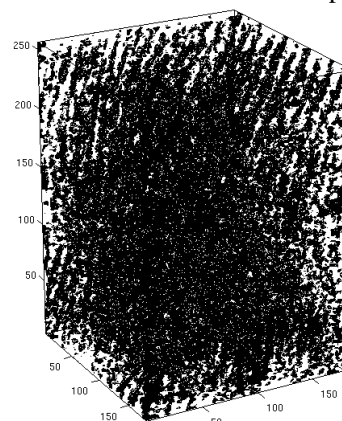


Fig.1: STIM-T reconstruction of a volume section of a butterfly wing: longitudinal ribs are perceived between outer and inner wing foils.

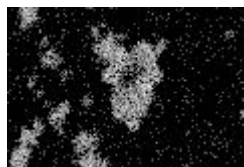
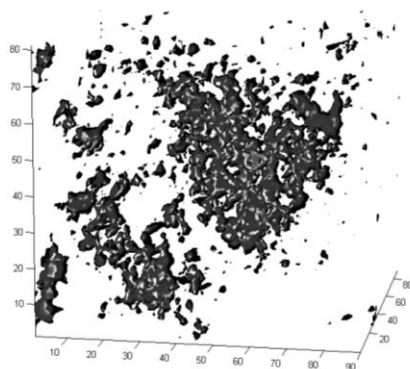


Fig.2: one of the Ni 2-D maps obtained by PIXE, and the resulting reconstruction showing the Ni inclusion 3-D pattern.



structural details *e.g.* sets of approximately equidistant longitudinal ribs. A test PIXE tomography experiment was also performed on a geological sample of a pyrite. The collection times were around 5 minutes per PIXE map. The reconstruction achieved using the same software was based in a set of $9+8$ 256×256 pixels Ni-distribution maps ($1060 \times 1060 \mu\text{m}^2$) and is shown in Fig.2: the Ni inclusion 3-D pattern becomes clearly visible.

Finally to run the reconstruction algorithm in a more user friendly way, a simple and practical single window interface was

developed, that considerably simplifies the data visualization after each reconstruction step.

As reconstruction quality and therefore the ability to distinguish such small structures are affected by the number of projection maps available, and this number also depends on time, use of interpolation between projection maps (acquired at consecutive angular positions) was attempted as a time saving tool. This expedient solution allowed some improvement of reconstruction based on fewer (approximately half) projection maps.